Formation and origin of the dominating electron trap in irradiated *p*-type silicon

Lasse Vines,[1,*] E. V. Monakhov,[1] A. Yu. Kuznetsov,[1] R. Kozłowski,[2] P. Kaminski,[2] and B. G. Svensson[1]
[1]*Department of Physics/Physical Electronics, University of Oslo, P.O. Box 1048 Blindern, N-0316 Oslo, Norway*
[2]*Institute of Electronic Materials Technology, PL-01919 Warsaw, Poland*
(Received 9 November 2007; revised manuscript received 19 May 2008; published 8 August 2008)

Deep level transient spectroscopy and minority-carrier transient spectroscopy (MCTS) have been applied to study electron-irradiated and proton-irradiated *p*-type Si samples with boron concentrations in the range of $6\times10^{13}-2\times10^{15}$ cm^{-3}. Both impurity-lean epitaxially grown samples and Czochralski grown samples have been investigated where some of the epitaxial samples were subjected to oxygenation prior to the irradiation in order to controllably vary the oxygen concentration. The MCTS measurements reveal a dominant electron trap at $E_c-0.25$ eV, where E_c is the conduction-band edge, commonly ascribed to a boron-interstitial oxygen-interstitial complex (B_iO_i). The amplitude of the level increases linearly with the irradiation dose and it anneals out at ~175 °C but shows, however, no correlation with the boron concentration. The level is dominant even at doping concentrations in the 10^{13} cm^{-3} range and, irrespective of the oxygen concentration, the generation rate decreases by almost 50% as the boron concentration increases by a factor of ~30. Comparison with numerical modeling reveals that these results are not consistent with the commonly accepted model of defect reactions in irradiated *p*-type Si. Different reasons for this discrepancy are discussed, such as an incomplete defect reaction model and alternative identifications of the $E_c-0.25$ eV level.

DOI: 10.1103/PhysRevB.78.085205 PACS number(s): 71.55.Cn, 61.80.Jh

I. INTRODUCTION

Electrically active point defects in silicon have been studied for several decades due to their fundamental importance and potential detrimental or beneficial effect on semiconductor devices. It is generally accepted that in irradiated *p*-type Si, the dominant hole traps are associated with the carbon-interstitial carbon-substitutional pair (C_iC_s), a defect originally identified by photoluminescence (PL) and electron-paramagnetic-resonance (EPR) studies,[1,2] the divacancy (V_2), a defect originally identified by EPR,[3] the carbon interstitial (C_i), initially identified by infrared-absorption spectroscopy studies,[4] and the carbon-interstitial oxygen-interstitial (C_iO_i) complex,[5] originally identified by optical and electrical techniques.[6] Further, the most prominent electron traps in *p*-type Si have been ascribed to C_i, C_iC_s,[1] and the boron-interstitial oxygen-interstitial pair (B_iO_i).[6] Specifically, the often dominating electron trap at $E_c-0.25$ eV, where E_c denotes the conduction-band edge, has been attributed to B_iO_i primarily because of an increase in intensity with increasing boron concentration and the abundance of O_i.[6–8] At sufficiently high boron concentrations, the intensity of the level decreases, which was attributed to the competing formation of the B_iB_s pair.[8] In recent theoretical work by Jones and co-workers,[9,10] and Sanati and Estreicher,[11] two forms of B_iO_i are predicted, indicating a more complex behavior of B-O clustering reactions than previously expected. However, the key arguments for an identification of the $E_c-0.25$ eV level as B_iO_i are the boron and oxygen dependencies.

In the current work, we employ deep level transient spectroscopy (DLTS) and minority-carrier transient spectroscopy (MCTS) to address the boron dependence of the $E_c-0.25$ eV level in electron-irradiated and proton-irradiated *p*-type samples with a relative variation in the boron concentration by a factor of 30. The samples used were mainly n^+pp^+ structures, accomplished by epitaxial growth and ion implantation, in order to ensure saturation of the MCTS peak intensities, which are known to be sensitive to the injection level of minority carriers. Indeed, in layers with high doping concentration, the injection is limited by the barrier height of the *pn* junction while in layers with low doping concentration, the injection can be limited by the series resistance.[12] In this respect, n^+pp^+ diodes with a thickness of the lightly doped layer, significantly smaller than the diffusion length of the minority carriers, such as in our structures, are ideal for measurements requiring a high and uniform injection level.

II. EXPERIMENT DETAILS

Mesa structured n^+pp^+ diodes were fabricated using pp^+ wafers where the *p* layer (~20 μm in thickness) was grown by chemical vapor deposition with a uniform boron doping concentration in the range of $6\times10^{13}-2\times10^{15}$ cm^{-3}, as deduced by capacitance-versus-voltage (CV) measurements. The p^+ substrate was Czochralski (Cz) grown with a boron concentration of $\sim5\times10^{18}$ cm^{-3}. The highly doped n^+ region was realized by a 36 keV P^+ ion implantation to a dose of 2×10^{14} cm^{-2} and subsequent activation annealing at 1050 °C for 10 min. For comparison, also n^+p diodes were fabricated using *p*-type Cz grown wafers with a boron doping concentration of 1.5×10^{15} cm^{-3}. For some selected epitaxial samples having 2×10^{15} B/cm^3, an oxygenation process[13,14] involving a dry oxidation for 8 h at 1100 °C followed by a heat treatment for 24 h at 1100 °C in N atmosphere, was carried out prior to the n^+-layer formation. The SiO_2 layer formed during the oxidation was subsequently removed by wet etching and CV measurements revealed a uniform carrier concentration identical within less than 20% compared to that in the nonoxygenated samples. Hence, ad-

ditional B doping by diffusion from the substrate is negligible as well as formation of electrically active centers by the in-diffused oxygen atoms. The latter result is consistent with that reported by other authors employing a similar oxygenation process[13] and suggests that the vast majority of the incorporated oxygen atoms occupy interstitial sites (O_i), as confirmed by infrared-absorption measurements.[15]

The oxygen and carbon chemical concentrations in the samples were measured by secondary-ion mass spectrometry (SIMS). The oxygen concentration in the Cz material was found to be about 1×10^{18} cm^{-3} while in the as-grown epitaxial layers, it increases from $\sim1\times10^{16}$ cm^{-3} in the surface region to 1×10^{17} cm^{-3} near the substrate. In the oxygenated epitaxial samples, a uniform oxygen concentration of 4×10^{17} cm^{-3} was observed through the whole thickness of the epitaxial layer. The carbon concentration in the Cz material was below the detection limit of $\sim5\times10^{16}$ cm^{-3}. This holds also for the epitaxial material, consistent with previous SIMS measurements by other authors, giving $[C]\lesssim8\times10^{15}$ cm^{-3} for the same kind of epitaxial samples[16] (brackets denote concentration values). No variation of [O] (and [C]) with the boron concentration in the samples was found.

Ohmic contacts to front and backside surfaces were formed by applying InGa and Ag pastes, respectively. For the Cz material, a 36 keV backside boron implantation was also carried out to improve the Ohmic contact.

The samples were irradiated at room temperature (RT) by 1.8 MeV protons having a penetration depth of ~40 μm, which is about twice (or more) the thickness of the epilayer. The doses used were between 2×10^{10} and 4×10^{12} cm^{-2}. In order to extract accurate values for the defect generation rates, each kind of sample was irradiated by three different doses. The probing depth in the DLTS measurements varies from 2.5 to 15 μm, depending on the dopant concentration, and the vacancy generation rate differs by 25% in this depth interval, as estimated by TRIM (Ref. 17) for 1.8 MeV protons. In addition, the epitaxial samples with low and high B concentrations were irradiated with 6 MeV electrons, using doses of 6×10^{13} and 2×10^{15} e$^-$/cm^2, respectively. After the RT irradiation, which lasted no more than 1 h, all the samples were stored at −20 °C until the initial DLTS/MCTS measurements were carried out followed by RT storage. Storage at −20 °C is sufficient to suppress, on the time scale of a few weeks, reactions involving migration of C_i.[18]

The DLTS/MCTS measurements were performed using a refined version of a setup described in detail elsewhere.[19] Both majority (DLTS) and minority (MCTS) carrier spectra were recorded. The minority-carrier injection was carried out by applying a forward bias of 3 V during the filling pulse while the capacitance transients were acquired at a reverse bias of −10 V for both the majority and minority-carrier measurements. In addition, capture cross-section measurements were undertaken by varying the duration of the filling pulse. The forward bias of 3 V was well above the threshold sufficient for saturation of the MCTS signal of the $E_c-0.25$ eV level, as illustrated by the inset of Fig. 1. The concentration of injected minority carriers was estimated by TCAD simulations using the commercially available SYNOPSYS software.[20] As illustrated in Fig. 1, for a forward bias of 3 V, the concentration of injected electrons in the epitaxial samples is calculated to be 2×10^{17} and 1×10^{16} cm^{-3} at RT and 100 K, respectively, while that in the bulk Cz samples is 2×10^{16} and 2×10^{15} cm^{-3}, respectively. Including a defect level at $E_c-0.25$ eV with electron and hole capture cross sections of 2×10^{-13} and 1×10^{-20} cm^2,[6] respectively, and a concentration of 10% of the doping concentration, the simulations yield a complete occupancy of the level during 3 V forward biasing at both 100 and 300 K, irrespective of the sample used. Thus, the simulations support the assumption of complete filling of E1 during MCTS and agree with the experimentally observed saturation of the amplitude of the $E_c-0.25$ eV level during MCTS. In addition, simulations of the MCTS spectra show that the influence of hole trapping by the V_2 level at $E_v+0.20$ eV on the $E_c-0.25$ eV level is negligible for the experimental conditions used (E_v denotes the valence-band edge). Thus, the concentration of the $E_c-0.25$ eV level can be deduced by the MCTS peak amplitude. The concentrations of the hole traps are found by the peak amplitudes in the DLTS spectra.

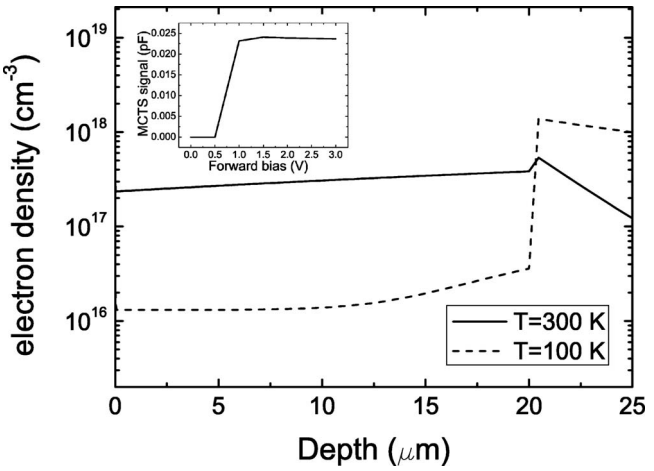

FIG. 1. Simulations of the steady-state electron density during the filling pulse in the MCTS measurements using a boron concentration of 2×10^{15} cm^{-3} and a forward bias of 3 V. The inset shows the measured MCTS intensity of the $E_c-0.25$ eV level versus forward bias pulse, illustrating the saturation of the MCTS signal.

III. RESULTS AND DISCUSSION

Figure 2 shows signatures of the hole traps detected by DLTS at $E_v+0.19$ eV (H1),[3] $E_v+0.30$ eV (H2)[4] and $E_v+0.36$ eV (H3),[5] attributed in accordance with literature to $V_2(+/0)$, C_i, and C_iO_i, respectively. In addition, a hole trap occurs at $E_v+0.42$ eV (H4). The material used in Fig. 2 is the most lightly doped one, $\sim6\times10^{13}$ B/cm^3, and H4 is barely present in the medium doped material and not detectable in the highly doped one, indicating that the trap is related to an impurity with low concentration such as hydrogen[21,22] or copper.[23] The H2 level, attributed to C_i, was observed during the first DLTS and MCTS scans after irradiation and −20 °C storage but then disappeared after a few days at RT in a 1:1 proportionality with the rise of the H3 level assigned to C_iO_i.

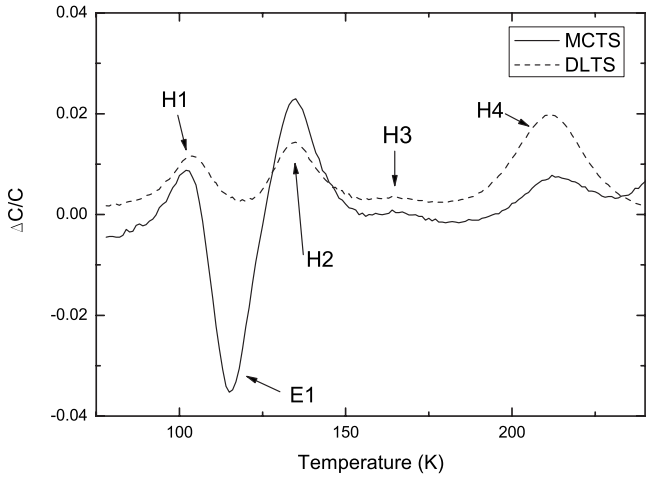

FIG. 2. Examples of normalized DLTS (dashed) and MCTS (solid) signals, $\Delta c/c$, taken from the proton-irradiated p-type epitaxial silicon samples having a doping concentration of 6×10^{13} B/cm^3. The rate window used is (640 ms)$^{-1}$.

Further, the electron trap at $E_c-0.25$ eV (E1 in Fig. 2), commonly assigned to B_iO_i, dominates the MCTS spectrum. The negative charge states of the divacancy $V_2(=/-)$ and $V_2(-/0)$, and the vacancy-oxygen (VO) pair are not observed due to their large hole capture cross section, promoting recombination rather than reemission of trapped electrons.[24] Overall, E1 is the dominating peak in Fig. 2, having a three times higher amplitude than that of $V_2(+/0)$. Isochronal annealing shows that E1 anneals out at ~175 °C (data not included), supporting that the E1 level is of the same origin as the $E_c-0.25$ eV level studied in Refs. 6–8.

Figure 3(a) reveals a linear dose dependence of the E1 intensities in the epitaxial samples. However, the generation rate, i.e., the slope of the E1 intensity versus dose, decreases with $[B_s]$. The corresponding concentration values of E1 are given in Table I. Although the average self-interstitial and vacancy generation rates within the measurement region decrease by ~25% from the low to the high doped sample, as estimated by TRIM calculations,[17] this difference is not sufficient to account for the observed dependence of the generation rate on $[B_s]$. In Fig. 3(b), which summarizes the boron concentration dependence of the generation rate for the defects observed in the epitaxial and Cz samples, the production of E1 is shown to decrease by almost 50% when $[B_s]$ increases from 6×10^{13} to 2×10^{15} cm^{-3} in the epitaxial samples. A similar trend, with a relative decrease by about 30%, is also found for the electron-irradiated samples (open symbols) where a highly uniform defect generation is expected. Figure 3(b) reveals also that (i) the generation rate of V_2 drops by 25% and hence stays constant with respect to the rate of vacancy generation, as estimated by the TRIM simulations, and (ii) the production of C_i decreases strongly with increasing $[B_s]$ because of the competition between C_s and B_s for capturing Si self-interstitials.[25] Furthermore, in the Cz samples, the generation rate of E1 is significantly reduced while $[C_i]$ has increased due to a higher carbon content in this material. In fact, the generation rate of E1 in the low doped epitaxial samples ($[B_s]\simeq6\times10^{13}$ cm^{-3}) is more

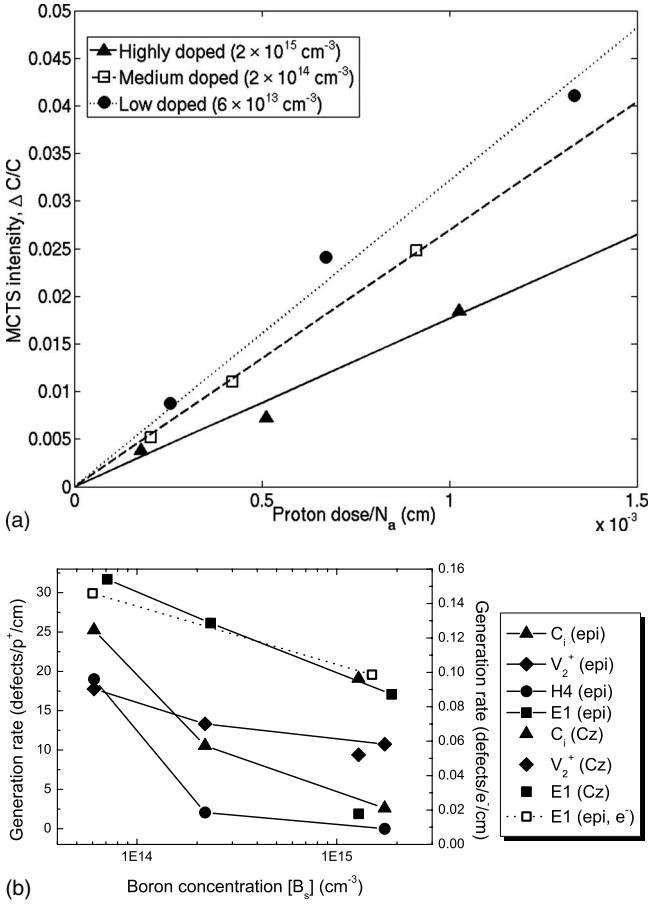

FIG. 3. (a) The dose dependence of the E1 signal as measured in the epitaxially grown samples. (b) Generation rate of the dominating point defects as a function of doping concentration for epitaxial (symbols+lines), and Cz (symbols) samples as measured after irradiation and storage at −20 °C. In addition, open symbols connected by a dashed line refer to the right ordinate and represent the results measured for the E1 level in electron-irradiated epitaxial material.

than one order of magnitude higher than that in the Cz material ($[B_s]\simeq1.5\times10^{15}$ cm^{-3}). This is in contrast to previous reports using bulk material showing no detection of E1 in lightly boron-doped samples.[6–8]

These different results imply that the formation of E1 hinges closely on the purity of the samples used. E1 is com-

TABLE I. Absolute concentration values of E1 in the different epi-materials used.

Proton dose (cm^{-2})	Lightly doped (cm^{-3})	Medium doped (cm^{-3})	Highly doped (cm^{-3})
2×10^{10}	6.8×10^{11}		
5×10^{10}	1.8×10^{12}	1.3×10^{12}	
1×10^{11}	3.1×10^{12}	2.6×10^{12}	
2×10^{11}		5.4×10^{12}	
3.5×10^{11}			7.4×10^{12}
1×10^{12}			1.4×10^{13}
2×10^{12}			3.2×10^{13}

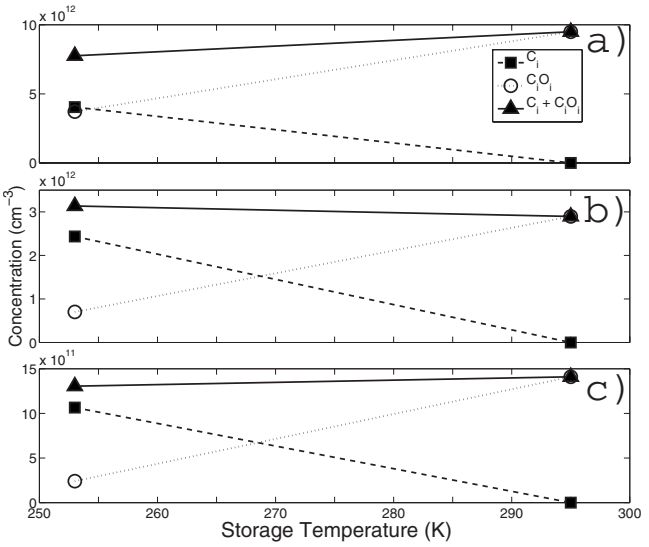

FIG. 4. Concentrations of C_i and C_iO_i (dotted lines), and their sum (solid line) measured after the −20 °C and RT storages for the highest irradiated dose in (a) 2×10^{15}, (b) 2×10^{14}, and (c) 6×10^{13} B cm^{-3} epitaxial samples. The time elapsed from the start of the irradiations at RT to the −20 °C storage was less than 1 h.

monly assigned to B_iO_i (Refs. 6–8) and the formation is primarily controlled by the following reactions:

$$I + B_s \rightarrow B_i, \tag{1}$$

$$I + C_s \rightarrow C_i, \tag{2}$$

$$B_i + O_i \rightarrow B_iO_i, \tag{3}$$

and

$$B_i + B_s \rightarrow B_iB_s. \tag{4}$$

In reaction (1), a Si self-interstitial (I) generated by the irradiation kicks out a B_s and the resulting B_i migrates until it encounters an O_i, forming the stable B_iO_i center [reaction (3)]. C_s is a main competitor to B_s for trapping of the migrating I's [reaction (2)] and the pronounced decrease in the generation rate of C_i when $[B_s]$ increases from 6×10^{13} to 2×10^{15} cm^{-3} [Fig. 3(b)], indicates that $[C_s]$ is only $\sim10^{14}$ cm^{-3} in the epitaxial layers, assuming similar capture radii of I by B_s ($R_I(B_s)$) and C_s ($R_I(C_s)$). According to the SIMS results, the oxygen content exceeds 10^{16} cm^{-3} in all the samples used, which suggests that $[O_i]\gg[B_s]$ and exhaustion of $[O_i]$ will not limit the formation of B_iO_i centers. However, at sufficiently high values of $[B_s]$ relative to that of $[O_i]$, the competing reaction (4) becomes important and enhances the generation of the B_iB_s pair on the expense of B_iO_i.

The C_i atoms generated by reaction (2) are known to be mobile at RT,[18] although slower than B_i, and can form stable centers with both O_i and C_s:

$$C_i + O_i \rightarrow C_iO_i \tag{5}$$

and

$$C_i + C_s \rightarrow C_iC_s. \tag{6}$$

As discussed above, it is anticipated that $[O_i]\gg[C_s]$ in the epitaxial samples and reaction (5) will dominate. Indeed, this is supported by the results in Fig. 4, showing, within the experimental accuracy, a 1:1 correlation between the loss of $[C_i]$ and the growth of $[C_iO_i]$ in all the samples.

A similar set of reactions as (1)–(6) has been considered in Ref. 28. In order to elucidate if these reactions can account for the experimentally determined generation rates of E1 and C_iO_i as a function of $[B_s]$ (Figs. 3 and 4), modeling has been performed. Applying the theory for diffusion-limited reactions,[29,30] the coupled differential rate equations derived from Eqs. (1)–(6) are given in Table II together with the input values used in the calculations. The differential equations are numerically solved simultaneously from time $t=0$, when the irradiation starts, until the defects have completed their reactions, which occurs long after the irradiation to a given fluence has finished. The ion flux used is 2×10^{10} H$^+$/cm^2 s, which is comparable with the experimental conditions. To comply with the concentration of I-related defects observed experimentally, a net generation rate of self-interstitials of ~75 I/(H$^+$ cm) is deduced from the lightly doped samples. A comparison with the total generation rate of I's, as estimated by TRIM calculations[17] assuming a displacement energy threshold of 15 eV, yields that only a fraction of ~1.5%–2% of the I's survive spontaneous (correlated) recombination with V's. Similar small fractions of surviving V's have previously been reported in low-dose ion-implanted *n*-type samples monitoring vacancy-type defects.[31]

The evolution in concentration of each stable defect center has been followed as a function of ion fluence in the range 10^{11}–10^{12} H$^+$/cm^2, and in this dilute regime, all the centers exhibit a linear dependence. From the slope of the defect concentration versus fluence, the generation rate per ion and unit length is extracted, and Fig. 5 shows a comparison between the simulated and experimental values for the different epitaxial samples studied. A close agreement is revealed for C_iO_i supporting the validity of reactions (1), (2), (5), and (6); here, it should be emphasized that the values used for $R_I(C_s)$ and $[C_s]_{t=0}$ are not unique but their product should remain constant relative to $R_I(B_s)[B_s]_{t=0}$ for a given value of $[B_s]_{t=0}$. Also B_iO_i and E1 display good agreement at low boron concentrations ($[B_s]\leq2\times10^{14}$ cm^{-3}) using a ratio between the capture radii $R_{B_i}(O_i)$ and $R_{B_i}(B_s)$ of ~0.018, i.e., this indicates that reaction (3) involves an energy barrier that exceeds the migration energy of B_i by ~0.1–0.2 eV if $R_{B_i}(B_s)$ is given by geometrical dimensions or, alternatively, $R_{B_i}(O_i)$ is given by the geometry while reaction (4) is enhanced because of attractive forces between B_i and B_s. However, for the highly doped epitaxial samples ($[B_s]\approx2\times10^{15}$ cm^{-3}), the calculated value of B_iO_i underestimates E1 by a factor of three and the generation of B_iB_s dominates strongly according to the simulations. Thus, the model exhibits a limited validity and does not fully account for the experimental data of E1. This conclusion is even more clearly illustrated by the results for the oxygenated epitaxial samples where the oxygen concentration is increased by more than one order of magnitude up to $\sim4\times10^{17}$ cm^{-3}. As shown in Fig. 6, the generation rate of

TABLE II. Survey of the simultaneous differential rate equations for the reactions in Eqs. (1)–(6) and numerical values of the input parameters used in the computations.

$$\frac{d[\mathrm{I}]}{dt} = g_{\mathrm{I}} - 4\pi D_{\mathrm{I}}[\mathrm{I}]\{R_{\mathrm{I}}(\mathrm{B}_s)[\mathrm{B}_s] + R_{\mathrm{I}}(\mathrm{C}_s)[\mathrm{C}_s]\}$$

$$\frac{d[\mathrm{B}_i]}{dt} = 4\pi D_{\mathrm{I}}[\mathrm{I}]R_{\mathrm{I}}(\mathrm{B}_s)[\mathrm{B}_s] - 4\pi D_{\mathrm{B}_i}[\mathrm{B}_i]\{R_{\mathrm{B}_i}(\mathrm{O}_i)[\mathrm{O}_i] + R_{\mathrm{B}_i}(\mathrm{B}_s)[\mathrm{B}_s]\}$$

$$\frac{d[\mathrm{B}_i\mathrm{O}_i]}{dt} = 4\pi D_{\mathrm{B}_i}[\mathrm{B}_i]R_{\mathrm{B}_i}(\mathrm{O}_i)[\mathrm{O}_i]$$

$$\frac{d[\mathrm{B}_i\mathrm{B}_s]}{dt} = 4\pi D_{\mathrm{B}_i}[\mathrm{B}_i]\mathrm{R}_{\mathrm{B}_i}(\mathrm{B}_s)[\mathrm{B}_s]$$

$$\frac{d[\mathrm{B}_s]}{dt} = -4\pi D_{\mathrm{I}}[\mathrm{I}]R_{\mathrm{I}}(\mathrm{B}_s)[\mathrm{B}_s] - 4\pi[\mathrm{B}_i]D_{\mathrm{B}_i}R_{\mathrm{B}_i}(\mathrm{B}_s)[\mathrm{B}_s]$$

$$\frac{d[\mathrm{C}_i]}{dt} = 4\pi D_{\mathrm{I}}[\mathrm{I}]R_{\mathrm{I}}(\mathrm{C}_s)[\mathrm{C}_s] - 4\pi D_{\mathrm{C}_i}[\mathrm{C}_i]\{R_{\mathrm{C}_i}(\mathrm{O}_i)[\mathrm{O}_i] + R_{\mathrm{C}_i}(\mathrm{C}_s)[\mathrm{C}_s]\}$$

$$\frac{d[\mathrm{C}_i\mathrm{O}_i]}{dt} = 4\pi D_{\mathrm{C}_i}[\mathrm{C}_i]R_{\mathrm{C}_i}(\mathrm{O}_i)[\mathrm{O}_i]$$

$$\frac{d[\mathrm{C}_i\mathrm{C}_s]}{dt} = 4\pi D_{\mathrm{C}_i}[\mathrm{C}_i]R_{\mathrm{C}_i}(\mathrm{C}_s)[\mathrm{C}_s]$$

$$\frac{d[\mathrm{C}_s]}{dt} = -4\pi D_{\mathrm{I}}[\mathrm{I}]R_{\mathrm{I}}(\mathrm{C}_s)[\mathrm{C}_s]$$

$$\frac{d[\mathrm{O}_i]}{dt} = -4\pi D_{\mathrm{B}_i}[\mathrm{B}_i]R_{\mathrm{B}_i}(\mathrm{O}_i)[\mathrm{O}_i] - 4\pi D_{\mathrm{C}_i}[\mathrm{C}_i]R_{\mathrm{C}_i}(\mathrm{O}_i)[\mathrm{O}_i]$$

Generation rate:	$g_{\mathrm{I}} = 1.5\times10^{12}$ cm^{-3} s^{-1} deduced from the experimental data with an ion flux of 2×10^{10} H$^+$/cm^2 s
Diffusion constants:	$D_{\mathrm{I}} = 1\times10^{-9}$ cm^2/s (rapid, see e.g. Ref. 26)
(300 K)	$D_{\mathrm{B}_i} = 1\times10^{-12}$ cm^2/s (taken from Ref. 27)
	$D_{\mathrm{C}_i} = 1\times10^{-15}$ cm^2/s (taken from Ref. 18)
Capture radii:	$R_{\mathrm{I}}(\mathrm{B}_s) = R_{\mathrm{B}_i}(\mathrm{B}_s) = R_{\mathrm{C}_i}(\mathrm{O}_i) = R_{\mathrm{C}_i}(\mathrm{C}_i) = 5$ Å (geometrical dimension)
	$R_{\mathrm{I}}(C_s) = 2.2$ Å, $R_{\mathrm{B}_i}(\mathrm{O}_i) = 0.09$ Å (fitted values)
Initial values ($t=0$):	$[\mathrm{C}_s] = 1\times10^{14}$ cm^{-3}, $[\mathrm{O}_i] = 1\times10^{16}$ cm^{-3} (4×10^{17} cm^{-3} after oxygenation)
	$[\mathrm{B}_s] = 5\times10^{13} - 5\times10^{15}$ cm^{-3}
	$[\mathrm{I}] = [\mathrm{B}_i] = [\mathrm{B}_i\mathrm{O}_i] = [\mathrm{B}_i\mathrm{B}_s] = [\mathrm{C}_i] = [\mathrm{C}_i\mathrm{O}_i] = [\mathrm{C}_i\mathrm{C}_s] = 0$

E1 after oxygenation remains essentially identical with that in the nonoxygenated samples while the simulations predict an increase of $\mathrm{B}_i\mathrm{O}_i$ by a factor of ~10, ~3, and ~1.3 in the highly, moderately, and lightly doped samples, respectively (Fig. 5). Here, it should also be pointed out that no deep level, such as the $E_v+0.30$ eV level observed in highly boron-doped bulk samples[6,7] and tentatively associated with the $\mathrm{B}_i\mathrm{B}_s$ pair, has been found to disappear or emerge on the expense of E1 in the epitaxial samples.

At least two possible reasons for the discrepancy between the commonly accepted model of defect reactions in irradiated *p*-type material, described by Eqs. (1)–(6), and the present experimental results for E1 can be put forward. First, E1 is correctly assigned to $\mathrm{B}_i\mathrm{O}_i$ but the model of defect reactions is incomplete. The lack of oxygen dependence indicates that $[\mathrm{O}_i] \sim 10^{16}$ cm^{-3} is sufficient to saturate the generation rate of E1 in the epitaxial samples but, on the other hand, a competing trap, which is boron-related and has a formation process with a stronger boron dependence than that of $\mathrm{B}_i\mathrm{O}_i$, must exist to account for the decrease in E1 with increasing $[\mathrm{B}_s]$. The $\mathrm{B}_i\mathrm{B}_s$ pair is one such candidate but it exhibits a too strong dependence when $[\mathrm{B}_s]$ is varied by a factor of 30, as shown in Fig. 5, and is not sufficient as the only competitor. No evidence for any additional boron-related and electrically active defect has been found in our measurements but a defect that is electrically inactive or escapes detection during the measurement conditions used cannot be excluded. Here, it may also be speculated that Fermi-level effects influence the net generation rate of surviving I's (and V's) although this appears to be inconsistent with the close agreement between the measured and simulated data for $\mathrm{C}_i\mathrm{O}_i$ in Fig. 5, as well as the essentially constant generation rate of V_2 versus $[\mathrm{B}_s]$ when accounting for the depth variations in elastic energy deposition. Second, a reidentification of E1 is discussed. The fact that E1 is not observed in *n*-type material suggest that it is either boron-related or its formation process is Fermi-level dependent. However, E1 is found in *n*-type samples counter doped with B,[32,33] indicating involvement of B and that the formation of E1 is not Fermi-level dependent. If B_i combines with an element, X, to form E1, the following considerations can be made: according to the DLTS spectrum of the sample irradiated with the highest dose [Fig. 3(a)], [E1], and thus [BX], is found to be $\sim3\times10^{13}$ cm^{-3}. Hence, [X] must be larger than 3×10^{13} cm^{-3}, assuming that [X] is the same in all the epitaxial samples. This implies that [X] is similar to or larger than

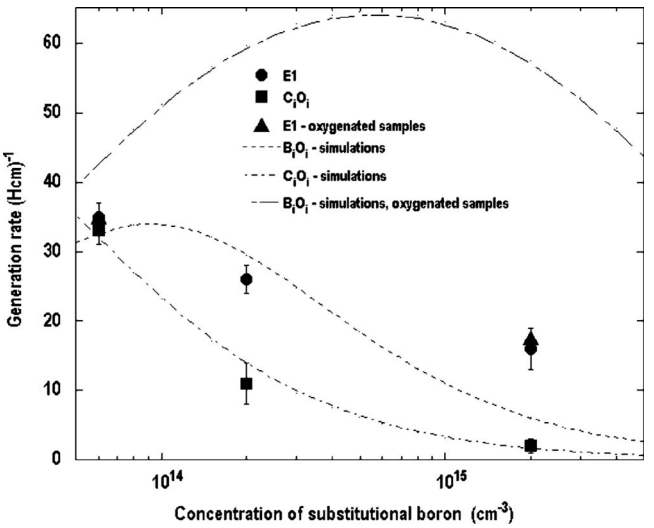

FIG. 5. Comparison between experimental values of the generation rate of C_iO_i and E1, and simulated ones for C_iO_i and B_iO_i as a function of $[B_s]$ in the epitaxial samples. The model used is described in the text and the numerical values for the input parameters are given in Table II. Results are also included for oxygenated epitaxial samples. Error bars indicate the experimental accuracy.

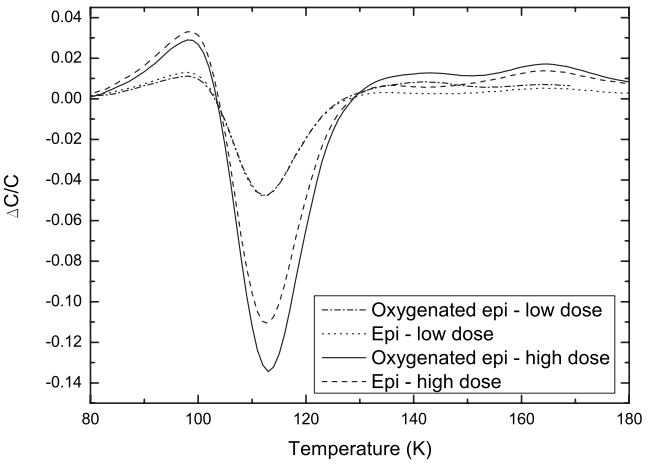

FIG. 6. MCTS spectra of oxygenated and nonoxygenated epitaxial samples ($[B_s] \simeq 2\times10^{15}$ cm^{-3}) irradiated by protons with low (2×10^{12} cm^{-2}) and high (4×10^{12} cm^{-2}) doses.

$[B_s]$ in the low doped material ($\sim 6\times10^{13}$ cm^{-3}). Possible candidates may then be boron-carbon related and boron-hydrogen related centers. Here, it should be clearly pointed out that such an assignment of E1 does not exclude the existence of B_iO_i; there is ample evidence for B_iO_i and recent theoretical predictions for local vibrational modes of the B_iO_i pair have been confirmed by experimental data.[34,35] Hence, in irradiated and oxygen-rich *p*-type samples, B_iO_i is, indeed, anticipated to play a major role, which favors an identification of E1 as B_iO_i. However, a reaction barrier B_i and O_i can suppress the absolute generation rate and other impurities/traps with concentrations substantially less than $[O_i]$ may become important.

IV. CONCLUSIONS

In conclusion, the generation rate of the dominant electron trap E1 ($E_c-0.25$ eV) in irradiated *p*-type silicon is found to decrease by $\sim$50% when the boron concentration increases by a factor of $\sim$30 from 6×10^{13} to 2×10^{15} cm^{-3} in carbon-lean epitaxial layers. Comparison with numerical modeling shows that these results are not consistent with the commonly accepted model of defect reactions in *p*-type Si and this conclusion is further substantiated by the fact that oxygenation of the epitaxial layers does not influence the generation rate of E1. Hence, further studies of the defect reactions taking place in irradiated *p*-type Si need to be pursued, including *in situ* DLTS studies of the B_i transition to E1 in samples with controlled carbon concentrations.

ACKNOWLEDGMENTS

This work was partly supported by the Norwegian Research Council through the NanoMat program and by the CERN RD50 collaboration.

*lassevi@fys.uio.no

[1] L. W. Song, X. D. Zhan, B. W. Benson, and G. D. Watkins, Phys. Rev. B **42**, 5765 (1990).
[2] L. W. Song, X. D. Zhan, B. W. Benson, and G. D. Watkins, Phys. Rev. Lett. **60**, 460 (1988).
[3] J. W. Corbett and G. D. Watkins, Phys. Rev. Lett. **7**, 314 (1961).
[4] A. R. Bean and R. C. Newman, Solid State Commun. **8**, 175 (1970).
[5] L. J. Cheng and P. Vadja, J. Appl. Phys. **40**, 4679 (1969).
[6] P. M. Mooney, L. J. Cheng, M. Süli, J. D. Gerson, and J. W. Corbett, Phys. Rev. B **15**, 3836 (1977).
[7] P. J. Drevinsky, C. E. Caefer, S. P. Tobin, J. C. Mikkelsen, and L. C. Kimerling, Mater. Res. Soc. Symp. Proc. **104**, 167 (1988).
[8] L. C. Kimerling, M. T. Asom, J. L. Benton, P. J. Drevinsky, and C. E. Caefer, Mater. Sci. Forum **38-41**, 141 (1989).
[9] J. Adey, R. Jones, and P. R. Briddon, Appl. Phys. Lett. **83**, 665 (2003).
[10] A. Carvalho, R. Jones, M. Sanati, S. K. Estreicher, J. Coutinho, and P. R. Briddon, Phys. Rev. B **73**, 245210 (2006).
[11] M. Sanati and S. K. Estreicher, Phys. Rev. B **72**, 165206 (2005).
[12] S. M. Sze, *Physics of Semiconductor Devices*, 2nd ed. (Wiley, New York, 1981), Chap. 2.4.3.
[13] L. Fonseca, M. Lozano, F. Campabadal, C. Martinez, M. Ullán, B. S. Avset, A. Ruzin, F. Lemeilleur, and E. Nossarzewska-Orlowska, Microelectron. Reliab. **40**, 791 (2000).

[14] G. Casse, CERN Technical Report No. ROSE/TN/99-1, 1999 (unpublished).
[15] M. Moll, E. Fretwurst, M. Kuhnke, and G. Lindström, CERN/LEB Technical Report No. 99-8, 1999 (unpublished); ROSE/RD48 Meeting, June 1999 (unpublished), pp. 51–80.
[16] I. Pintilie, M. Buda, E. Fretwurst, G. Lindström, and J. Stahl, Nucl. Instrum. Methods Phys. Res. A **556**, 197 (2006).
[17] J. F. Ziegler, J. P. Biersack, and U. Littmark, *The Stopping and Range of Ions in Solids* (Pergamon, New York, 1985).
[18] A. K. Tipping and R. C. Newman, Semicond. Sci. Technol. **2**, 315 (1987).
[19] B. G. Svensson, K.-H. Rydén, and B. M. S. Lewerentz, J. Appl. Phys. **66**, 1699 (1989).
[20] Synopsys Inc., 700 East Middlefield Road, Mountain View, California 94043, USA; see also http://www.synopsys.com/
[21] O. Feklisova, N. Yarykin, E. B. Yakimov, and J. Weber, Physica B (Amsterdam) **308-310**, 210 (2001).
[22] S. Fatima, C. Jagadish, J. Lalita, B. G. Svensson, and A. Hállen, J. Appl. Phys. **85**, 2562 (1999).
[23] S. D. Brotherton, J. R. Ayres, A. Gill, H. W. van Kesteren, and F. J. A. M. Greidanus, J. Appl. Phys. **62**, 1826 (1987).
[24] A. Hallén, N. Keskitalo, F. Masszi, and V. Nágl, J. Appl. Phys. **79**, 3906 (1996).
[25] R. D. Harris, J. L. Newton, and G. D. Watkins, Phys. Rev. B **36**, 1094 (1987).
[26] G. S. Oehrlein, I. Krafczik, J. L. Lindström, A. E. Jaworowski, and J. W. Corbett, J. Appl. Phys. **54**, 179 (1983).
[27] A. K. Tipping and R. C. Newman, Semicond. Sci. Technol. **2**, 389 (1987).
[28] S. Zhao, A. M. Agarwal, J. L. Benton, G. H. Gilmer, and L. C. Kimerling, Mater. Res. Soc. Symp. Proc. **442**, 231 (1997).
[29] T. R. Waite, Phys. Rev. **107**, 463 (1957).
[30] T. R. Waite, J. Chem. Phys. **28**, 103 (1958).
[31] B. G. Svensson, C. Jagadish, A. Hallén, and J. Lalita, Phys. Rev. B **55**, 10498 (1997).
[32] J. R. Troxell and G. D. Watkins, Phys. Rev. B **22**, 921 (1980).
[33] V. P. Markevich (private communication).
[34] A. Carvalho, R. Jones, J. Coutinho, and P. R. Briddon, J. Phys.: Condens. Matter **17**, L155 (2005).
[35] L. I. Murin, V. P. Markevich, J. L. Lindström, and B. G. Svensson (unpublished).